Heterogeneous current collector in lithium-ion battery for thermal-runaway mitigation

Meng Wang,[1] Anh V. Le,[1] Yang Shi,[2] Daniel J. Noelle,[2] and Yu Qiao[1,2,a)]
[1]*Department of Structural Engineering, University of California–San Diego, La Jolla, California 92093-0085, USA*
[2]*Program of Materials Science and Engineering, University of California–San Diego, La Jolla, California 92093, USA*

(Received 7 December 2016; accepted 23 January 2017; published online 21 February 2017)

Current collector accounts for more than 90% of the electric conductivity and ~90% of the mechanical strength of the electrode in lithium-ion battery (LIB). Usually, current collectors are smooth metallic thin films. In the current study, we show that if the current collector is heterogeneous, the heat generation becomes negligible when the LIB cell is subjected to mechanical abuse. The phenomenon is attributed to the guided strain concentration, which promotes the separation of the forward and the return paths of internal short circuit. As the internal impedance drastically increases, the stored electric energy cannot be dissipated as thermal energy. The modification of current collector does not affect the cycling performance of the LIB cell. This finding enables advanced thermal-runaway mitigation techniques for high-energy, large-scale energy storage systems. *Published by AIP Publishing*. [http://dx.doi.org/10.1063/1.4975799]

Lithium-ion battery (LIB) has been studied intensively for years. Compared with other energy storage devices such as lead-acid batteries and supercapacitors, LIB has a high specific energy and a low specific cost.[1] Currently, as much effort is spent on enhancing the energy and cycling performance of LIB,[2,3] increasing attention is drawn to its safety.

Large-scale energy storage is an emerging application of LIB. Examples include electric vehicles (EVs) and smart grids.[4,5] Because lithium is reactive with water, the electrolyte in LIBs must be based on non-aqueous organic solvents, typically ethyl methyl carbonate (EMC), dimethyl carbonate (DMC), or diethyl carbonate (DEC). These solvents are highly flammable and volatile;[6] their flashing points are around room temperature, responsible for many fire cases of EVs and LIB cells (e.g., Ref. 7). As a battery is being discharged, electric energy would be dissipated and the cell temperature would increase. Under ordinary working condition, the heat generation is mild.[8] In an accident when the LIB cell is damaged, however, catastrophic failure may take place. For instance, when the battery cell is subjected to a blunt impact, the cell case would deform and the membrane separator may be ruptured. Thus, a conductive path is internally formed between the cathode and the anode, causing internal shorting. The forward path is for the electron motion from the anode to the cathode, either through the foreign conductive penetrator or directly across the cathode-anode interface; the return path is through the ionic conduction in surrounding area. If the heat generation rate exceeds the heat transfer rate, the local temperature at shorting site, T, would increase. When T reaches ~110 °C, a number of secondary reactions would be activated, including the decomposition of electrolyte and electrodes. These exothermal reactions are accelerated as T further rises, eventually leading to thermal runaway. As a result, the local temperature can rapidly increase by several hundred Celsius in a fraction of minute.[9]

In order to optimize the battery cell performance, the cathode and the anode must be placed in close proximity, separated by a thin porous polymer film of 10–30 μm thickness. The choice of the membrane separator material is constrained by the cost, the stability, the porosity, etc., and usually polypropylene or polyethylene is employed. The membrane separators are relatively fragile, and therefore, the forward path of internal shorting can be quite easily formed as the cell case deforms.

Over the years, a few techniques were studied to block the return path of internal short circuit. The rate of heat generation may be assessed as $Q = U^2/R$, where U is the electrode voltage and R is the internal impedance. To maintain a low internal impedance under normal condition while drastically increase it in an event of battery damage, one way is to use positive thermal coefficient (PTC) additives,[10,11] e.g., monomers that can be polymerized at an elevated temperature. A major issue of this approach is the relatively slow reaction rate. Another method is to use low-melting-point membrane separators:[12] When temperature increases, the separator melts and blocks ion conduction; however, it does not solve the problem if the membrane is ruptured, especially for high-energy and large energy storage units. Furthermore, the above thermal-runaway mitigation mechanisms are thermally triggered. The triggering temperature must be much higher than the operation/storage temperature range of LIB, around 110–130 °C, which is already at the critical point of thermal runaway (~120 °C). Recently, we investigated damage homogenizers (DM), such as carbon black microparticulates and carbon nanotube bundles.[13–15] As ~1% DM is mixed in electrode, the active material layer is weakened. When an external loading is applied, widespread damaging could take place. Hence, the internal impedance increases, and the risk of thermal runaway is reduced. Such a process is

a)Author to whom correspondence should be addressed. Electronic mail: yqiao@ucsd.edu. Tel.: +1(858)534-3388. Fax: +1 (858) 534-1310.

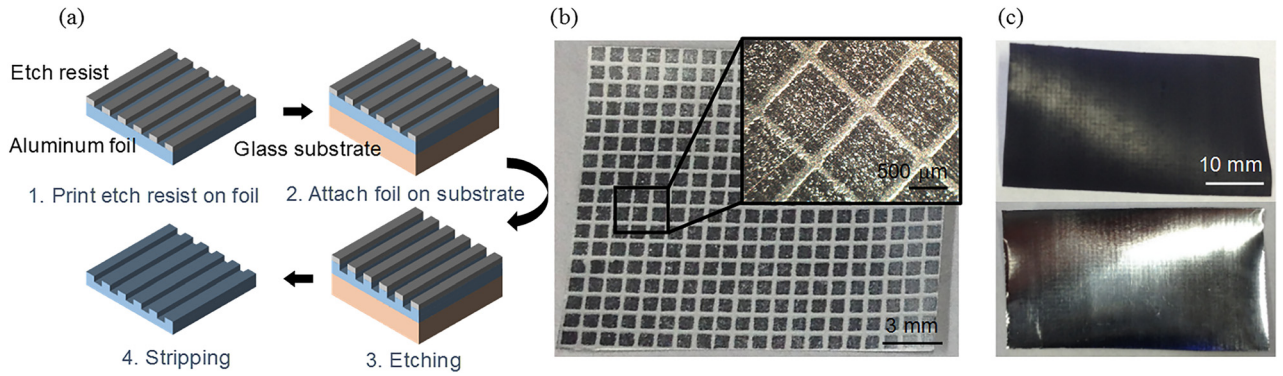

FIG. 1. (a) Processing of current collector. (b) Photos of modified current collector. (c) Top and bottom views of modified current collector with electrode coating.

mechanically triggered. It can take effect simultaneously as the LIB cell damage occurs, before the cell temperature starts rising.

An LIB electrode contains at least two layers, the active material layer and the current collector. The active material layer is typically coated onto the current collector with the thickness ranging from 10 to 100 μm; the current collector is often an aluminum (Al) or copper (Cu) sheet, with the thickness around 10 to 20 μm. Internal shorting through current collectors is much more dangerous than through active material layers,[16] since current collector accounts for more than 90% of electric conductivity and ~90% of mechanical strength of the electrode. If the current collector can be modified so that it is a continuous piece during normal operation while under mechanical abuse condition, it would fracture into discontinuous pieces, the internal shorting site can be completely isolated from the surrounding electrode area. Hence, internal impedance can be significantly increased, leading to a much lower heat generation rate.

In the current study, current collector was modified to be heterogeneous (Fig. 1(a)). Finished current collector is shown in Fig. 1(b). After slurry coating and calendering, the surface flatness of current collector was not affected (Fig. 1(c)). The details of processing of current collector and electrode are given in Sections S1 and S2 in the supplementary material, respectively.

The electric conductivity of aluminum current collector is 3.8×10^5 S/m, five orders of magnitude higher than that of active material (NMC532).[9] In an internal short circuit, the current collector contributes to most of the heat generation. The stiffness and the strength of the electrode are also largely determined by the current collector. As shown in Table S1 in the supplementary material, the aluminum current collector has a high stiffness of ~70 GPa (compared to ~0.05 GPa of NMC532) and a high strength ~165 MPa (compared to ~1.7 MPa of NMC532 (Ref. 17)). To promote the isolation of internal short circuit and to increase the internal impedance, modifying current collector should be more efficient than weakening the active material layer.

Modified LIB half-cells with heterogeneous current collectors and reference half-cells with smooth current collectors were characterized in impact tests. The details of LIB cell processing and testing are given in Sections S3 and S4 in the supplementary material, respectively. In an impact test, as the upper rod is dropped on the lower rod, the indenter was intruded into the electrode stack (Fig. 2(a)). For selected cells, the electrode layers were de-assembled and inspected. Fig. 2 shows typical photos of impacted reference current collectors. It can be observed that when subjected to the intense impact loading, both separator and current collector are ruptured. A few radial cracks are formed from the impact site and propagate into the far field, exhibiting a typical failure mode of dynamic penetration of thin films.[18] The anode lithium disc is in direct contact with the NMC532 layer as well as the deformed, fractured current collector sectors. As a result, internal shorting happens and the stored electric energy is rapidly dissipated as heat, leading to the temperature increase shown in Fig. 2(b). The heat generation is reflected in the temperature profiles. In the first few seconds following the formation of internal short circuit, heat generation dominates the temperature change, $Q = mc\Delta T$, where m is the cell mass, c is the effective heat capacity, and ΔT is the temperature increase. The peak temperature increase of the reference cell, ΔT_{ref}, is ~5 °C, which is reached in about half a minute, followed by a plateau wherein the heat generation and heat transfer are balanced. Eventually, after about 1.5 min, the energy of half-cell is largely consumed and the heat generation rate decreases, causing the relatively long tail region in the temperature profile.

We also tested a few fully discharged reference half-cells. Although no electric energy was stored, due to rupture, friction, and plastic yielding associated with the dissipation of kinetic energy of drop mass, the thermocouple detected a mild temperature increase, about 30% of ΔT_{ref}.

According to Fig. 2(c), the failure mode of heterogeneous current collector is fundamentally different from that of smooth current collector. At the point of impact, i.e., the center of the current collector, the current collector is entirely truncated from the surrounding electrode; that is, the forward path of internal short circuit is connected to the return path by only the NMC532 layer, not through the highly conductive current collector. Consequently, the internal impedance is much increased, and the heat generation rate is reduced. The increase in the resulting temperature, ΔT, is around 30% of ΔT_{ref}, close to that of a fully discharged half-cell, suggesting that the heat generation associated with internal shorting is negligible.

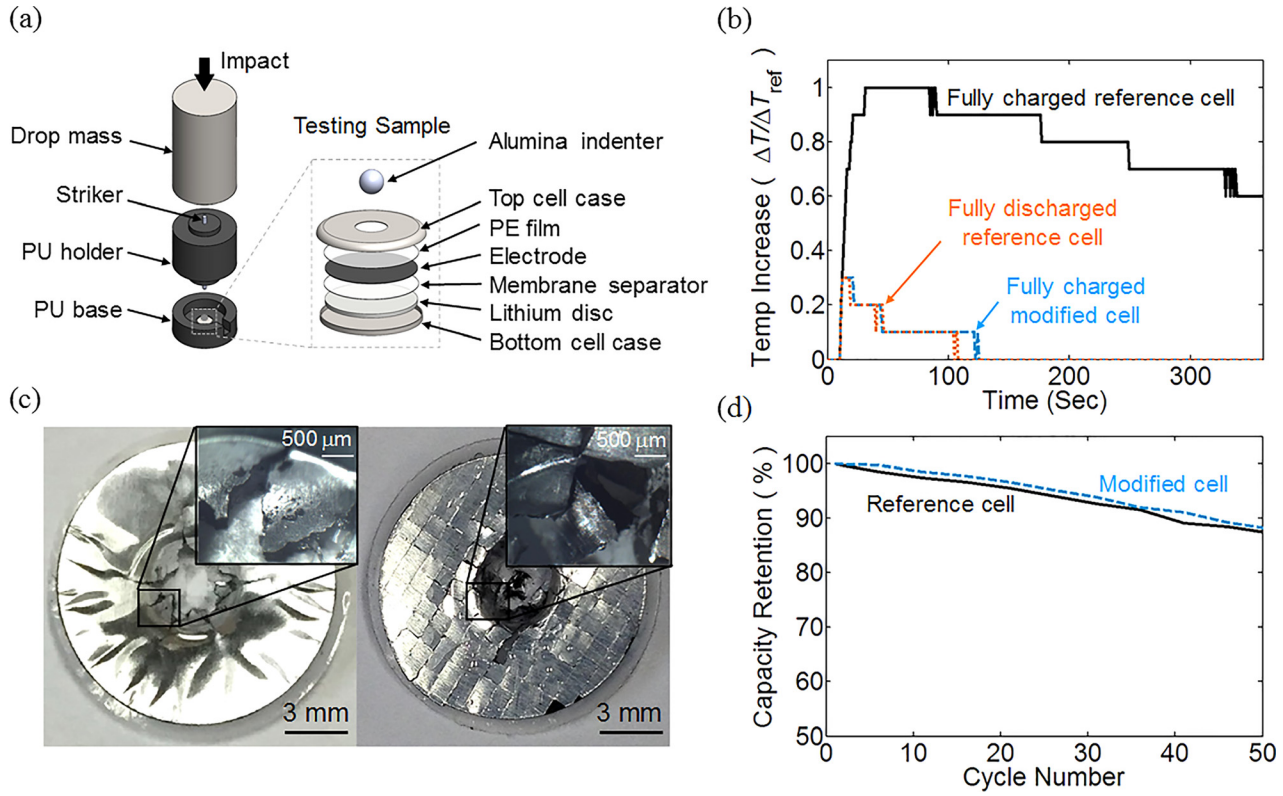

FIG. 2. (a) Schematic of the impact testing setup. (b) Typical cell surface temperature profiles in impact experiment. (c) Photos of reference (left) and modified (right) current collectors after impact testing. (d) Typical cycling performance of reference and modified battery cells.

The difference in the failure modes of reference and modified current collectors should be attributed to the heterogeneity. Upon impact, crack propagation is highly influenced by the local material properties and geometry. At the intersections of the surface groove network, crack bifurcation is promoted, and, instead of radial crack growth, a complete concentric crack is formed surrounding the crack nucleation site. Like a fully discharged cell, peak temperature of a modified LIB cell is reached in a few seconds and the heat is dissipated in ~2 min.

The state of charge measurement results are consistent with the above analysis: If the cathode is based on smooth current collector, after impact, the residual voltage is 2.00 ± 0.4 V; if the cathode is based on heterogeneous current collector, the residual voltage is 4.54 ± 0.1 V, only slightly lower than the initial value. Because simultaneously as the cell is impacted, the damaged region is isolated from the rest of the LIB, a large portion of the NMC532 layer in a modified cell is not fully discharged.

Fig. 2(d) shows the capacity retention of the coin cells during cycling tests. The cycling experiment was conducted at 1C rate from 3 V to 4.3 V. The initial capacity was around 148 mA h/g, with the active material loading of ~17.4 mg/cm^2. The behaviors of reference and modified cells are nearly the same, which is as expected because the modification of current collector geometry does not affect the electrochemical reactions. We observed that the adhesion between the modified current collector and the NMC532 layer was stronger, probably due to the increase in effective contact area.

A finite element analysis (FEA) was conducted to further understand the failure modes of smooth and heterogeneous current collectors (Fig. 3). As the current collector is smooth, cracks propagate along radial directions, and the sectors in between the radial cracks are bent downward, contacting the lithium disc. Consequently, the entire cathode layer is involved in the short circuit. When the current collector contains surface grooves, crack propagation is guided to the weakened routes. The plastic-strain concentration at the perimetric grooves near the impact site triggers crack bifurcation, causing the formation of concentric crack. The central piece of the heterogeneous current collector is entirely broken off. Thus, the electric conductivity between the internal shorting site and the rest of electrode area is drastically decreased.

Fig. 3(c) shows the evolution of the plastic strain fields in reference and modified current collectors, as the indenter displacement increases. In the reference current collector, the plastic deformation is focused around the indentation site. In the near field, the plastic strain distribution is relatively homogeneous; in the far field, the plastic strain is negligible. Even when the indenter moves deep into the current collector, the maximum strain is still lower than the critical value of final failure. That is, the damage mechanism of reference current collector is mainly plastic deformation and radial cracking. The modified current collector demonstrates a different procedure: The plastic strain is "guided" by the surface grooves and extends to the far field, even in the early stage of impact. Nearly all the plastic deformation is concentrated at the groove roots, and the areas in between the grooves deform elastically. As the fracture along grooves causes the separation of central piece, the forward path of internal short circuit is isolated, consistent with the experimental observation.

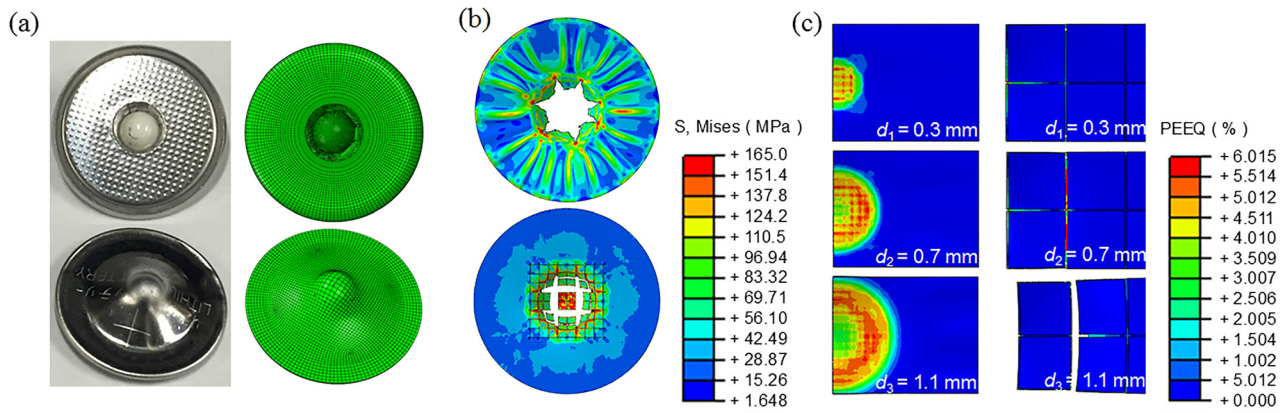

FIG. 3. (a) Top and bottom views of the experimental (left) and the computer simulation (right) results of impacted battery cell. (b) Cracking modes of reference (top) and modified (bottom) current collectors. (c) Plastic-strain distributions in reference (left) and modified (right) current collectors, where d_i ($i = 1$, 2, or 3) is the indenter displacement.

To conclude, we modified the current collector in lithium-ion battery, so as to mitigate thermal runaway when the battery cell is impacted. The mechanism is mechanically triggered, independent of the cell temperature; that is, it can be activated immediately after the cell is deformed, before the cell temperature starts to rise. The modification is achieved by creating heterogeneous features on the surface of current collector, which act as plastic-strain concentrators leading to the formation of concentric crack. Consequently, the forward path of internal short circuit is separated from the return path, and the internal impedance increases significantly. The impact testing data indicate that, with the heterogeneous current collector, when the battery cell is subjected to mechanical abuse, the temperature increase caused by internal shorting is negligible. This technique is relevant to large-scale energy storage structures working under harsh conditions.

See supplementary material for the details of electrode processing (Section S1), current collector modification (Section S2), coin cell fabrication (Section S3) and testing (Section S4), and finite element modeling (Section S5).

This research was supported by the Advanced Research Projects Agency-Energy (ARPA-E) under Grant No. DE-AR0000396, for which we are grateful to Dr. Ping Liu, Dr. John Lemmon, Dr. Grigorii Soloveichik, Dr. Chris Atkinson, and Dr. Dawson Cagle. Special thanks are also due to Professor Y. Shirley Meng, Dr. Hyojung Yoon, and Mr. Minghao Zhang for their help with the battery cell processing.

[1]B. Scrosati and J. Garche, J. Power Sources **195**, 2419–2430 (2010).
[2]H. L. Wang, L. F. Cui, Y. A. Yang, H. S. Casalongue, J. T. Robinson, Y. Y. Liang, Y. Cui, and H. J. Dai, J. Am. Chem. Soc. **132**, 13978–13980 (2010).
[3]Y. Wang and G. Z. Cao, Adv. Mater. **20**, 2251–2269 (2008).
[4]M. M. Thackeray, C. Wolverton, and E. D. Isaacs, Energy Environ. Sci. **5**, 7854–7863 (2012).
[5]S. B. Peterson, J. Apt, and J. F. Whitacre, J. Power Sources **195**, 2385–2392 (2010).
[6]C. Arbizzani, G. Gabrielli, and M. Mastragostino, J. Power Sources **196**, 4801–4805 (2011).
[7]Q. S. Wang, P. Ping, X. J. Zhao, G. Q. Chu, J. H. Sun, and C. H. Chen, J. Power Sources **208**, 210–224 (2012).
[8]R. Sabbah, R. Kizilel, J. R. Selman, and S. Al-Hallaj, J. Power Sources **182**, 630–638 (2008).
[9]S. Santhanagopalan, P. Ramadass, and J. Zhang, J. Power Sources **194**, 550–557 (2009).
[10]G. Venugopal, J. Power Sources **101**, 231–237 (2001).
[11]M. Baginska, B. J. Blaiszik, R. J. Merriman, N. R. Sottos, J. S. Moore, and S. R. White, Adv. Energy Mater. **2**, 583–590 (2012).
[12]P. Arora and Z. M. Zhang, Chem. Rev. **104**, 4419–4462 (2004).
[13]A. V. Le, M. Wang, Y. Shi, D. Noelle, Y. Qiao, and W. Y. Lu, J. Appl. Phys. **118**, 085312 (2015).
[14]A. V. Le, M. Wang, Y. Shi, D. J. Noelle, and Y. Qiao, J. Phys. D: Appl. Phys. **48**, 385501 (2015).
[15]M. Wang, A. V. Le, Y. Shi, D. J. Noelle, H. Yoon, M. Zhang, Y. S. Meng, and Y. Qiao, J. Mater. Sci. Technol. **32**, 1117–1121 (2016).
[16]W. Zhao, G. Luo, and C. Y. Wang, J. Electrochem. Soc. **162**, A1352–A1364 (2015).
[17]P. Liu, E. Sherman, and A. Jacobsen, J. Power Sources **189**, 646–650 (2009).
[18]R. Vermorel, N. Vandenberghe, and E. Villermaux, Phys. Rev. Lett. **104**, 175502 (2010).

SUPPLIMENTARY MATERIAL

for

Heterogeneous Current Collector in Lithium-Ion Battery for Thermal-Runaway Mitigation

Meng Wang,[1] Anh V. Le,[1] Yang Shi,[2] Daniel J. Noelle,[2] Yu Qiao[1,2,*]

[1] *Department of Structural Engineering, University of California – San Diego, La Jolla, CA 92093-0085, U.S.A.*
[2] *Program of Materials Science and Engineering, University of California – San Diego, La Jolla, CA 92093, U.S.A.*

[*] Corresponding author. Phone: +1(858)534-3388; Fax: +1 (858) 534-1310. Email: yqiao@ucsd.edu

S1. Electrode processing

In the current study, Toda $LiNi_{0.5}Mn_{0.3}Co_{0.2}O_2$ (NMC532) was employed as the active material of cathode; TIMCAL C-NERGY Super-C65 carbon black (CB) was added as the conductive filler; and polyvinylidene fluoride (PVDF, obtained from Sigma-Aldrich) was used as the binding material. The mass ratio of NMC532, CB and PVDF was 93:3:4. The powders were manually mixed in a mortar using a pestle for 30 min. Slurry was produced by manually mixing 10 g of powders with 4 ml 1-Methyl-2-pyrrolidone (NMP). The slurry was homogenized using a Qsonica Q55 sonicator at the power level 70 for 15 min, and coated onto a modified or reference MTI aluminum (Al) current collector, by a MTI Micrometer Adjustable Film Applicator (EQ-Se-KTQ-100). The gap of coating was set to 200 μm. The coated slurry was dried in a vacuum oven at 80 ^oC for 24 hours and the electrode thickness was reduced to about 100 μm. It was compressed by a rolling press to the final thickness of ~80 μm, and punched into 14.3-mm-diameter circular pieces.

S2. Current collector processing

Prior to the slurry processing, the current collector had been modified through etching. The as-received current collector was smooth 18-μm-thick aluminum (Al) foil. It was repeatedly rinsed by acetone and de-ionized water, dehydrated at 150 ^oC for 20 min, and affixed onto a 3M GG3300 polymer substrate by Kapton tapes. Etch resist was directly printed onto the current collector by a HP Jetpro400 laser printer with a heterogeneous pattern. The pattern consisted of two sets of straight lines perpendicular to each other, with the line width and spacing of ~100 μm and ~1 mm, respectively. Then, the current collector was dried in a gravity oven at 100 ^oC for 20 min, and etched in Transene Type-A Al Etchant at 50 ^oC for 20 min, followed by repeated dip-rinsing in acetone and isopropyl alcohol. The surface of the etched current collector was characterized by a Zygo NewView 600 Surface Profiler, and the width and the depth of the surface grooves were measured as ~100 μm and ~14 μm, respectively. The back surface of the current collector remained smooth. Reference cathodes were processed on un-modified current collectors.

S3. Coin cell processing

Type-2016 half-cell was assembled in a MBRAUN Glove Box in argon environment (H_2O < 0.5 ppm), using the produced cathode, a 15.4-mm-diameter 1.1-mmthick lithium disc as the anode, a Celgard 2320 PP-PE-PP membrane as the separator, and Type-2016 stainless steel cell case. Before the cell case was sealed by the hydraulic crimping machine (MTI, MSK-110), 30 µL BASF electrolyte (1M $LiPF_6$ in 1:1 EC-EMC) was added. The cell was rested for 12 h before testing.

S4. Coin cell testing

The cycling performances of the reference cells with smooth current collectors and the modified cells with heterogeneous current collectors were characterized by using an eight-channel battery analyzer (BST8-MA). The charging rate was 1 C and the voltage range was 3 V to 4.3 V.

To investigate the heat generation behavior upon mechanical abuse, half-cells were charged to 4.6 V by a MTI BST8-3 Battery Analyzer, with the charging rate of C/10. The cell case was opened; a 15.4-mm-diameter 150-µm-thick polyethylene (PE) film was placed on top of the cathode; the layer stack was then fastened by a modified stainless steel cover with a 6.35-mm-diameter hole in the center. The fully charged half-cell was firmly held by a 76.2-mm-diameter 12.7-mm-thick circular support, made from 90A hard solid polyurethane (PU). The support had a matching hole that hosted the half-cell. At the center of the top surface of the half-cell, a 4.8-mm-diameter alumina ball was placed; it served as the indenter. The top of the cell was insulated by a layer of 1-mm-thick porous PU sheet with duct tapes. A 4.8-mm-diameter 127-mm-long stainless steel lower rod penetrated through the PU sheet and rested on the indenter. A 304.8-mm-long 63.5-mm-diamter steel rod was dropped onto the lower rod, with the drop distance of 5 cm; the drop mass was 7.8 kg. A type-K thermometer was attached to the upper surface of the battery cell, 5 mm away from the center, and connected to an Omega OM-EL-USB-TC temperature logger; the data sampling frequency was 1 Hz.

After the impact test, the cell was disassembled to determine their state of charge. The tested cathode was taken out in the glovebox, and assembled into a new cell with new separator, lithium disc, and cell case. The voltage of the re-assembled cell was measured by a multimeter (B&K Precision 2405A).

S5. Finite element modeling

Finite element analysis (FEA) was conducted by the ABAQUS Explicit package, using eight-node solid elements with reduced integration (C3D8R). The computer simulation model contained a rigid spherical indenter, placed on a layer stack of the current collector, the lithium disc, and the bottom cell case. The NMC532 layer was ignored, since its stiffness and strength were much lower than those of current collector (Table S1). The interaction between the current collector and the lithium disc was modeled by general contact with a penalty function; the friction coefficient was taken as 0.3. The shapes, sizes, and materials of the cell components were identical to those of testing sample. The mechanical properties were from [S1, S2] as well as the materials manufacturer (MTI). In

the reference sample, the current collector was smooth. In the modified sample, the central part of the current collector contained surface grooves with the same dimension as in experiment. The cross section of the grooves was rectangle, with the depth of 14 μm and the width of 100 μm. Through a mesh sensitivity analysis, the FEA mesh size of current collector was set to 20-40 μm; the FEA mesh sizes of indenter, lithium disc, and cell case were 160 μm, 160 μm and 320 μm, respectively.

The rigid indenter was intruded into the layer stack with the initial speed of 1 m/s and a linear deceleration of 78.7 m/s^2. The cell case and the lithium disc were modeled as linear elastic-plastic materials. For the current collector, both linear elastic-plastic and damage models were investigated. The damage initiation criteria were based on the maximum strain. After the maximum strain of an element was reached, the element would be deleted from the global meshing. At the lateral and the bottom boundaries, all degrees of freedom were fixed; the top surface was free.

Table S1. Mechanical properties of cell components

Cell Components	Material	Modulus of Elasticity (GPa)	Poisson's ratio	Yield Strength (MPa)	Ultimate Tensile Strength (MPa)	Failure strain (%)
Cathode active material	NMC532	0.05	N/A	0.9	1.7	20
Cathode current collector	1235 H18 aluminum	69	0.33	151.7	165.5	5
Anode	Lithium	7.8	0.36	0.85	1.38	6.4
Cell case	304 stainless steel	197	0.29	215	505	70

References

[S1] P. Liu, E. Sherman and A. Jacobsen, J Power Sources **189**, 646-650 (2009).

[S2] S. Tariq, K. Ammigan, P. Hurh, R. Schultz, P. Liu and J. Shang, in *Proc. Particle Accelerator Conf. 2003 (ISSN 1063-3928)*, May 12-16, 2003.